# Spontaneous decay rate of an excited molecule placed near a circular aperture in a perfectly conducting screen: An analytical approach

Vasily V. Klimov,[1,2,3,*] Dmitry V. Guzatov,[4] and Ilya V. Treshin[1,2]

[1]*P. N. Lebedev Physical Institute, Russian Academy of Sciences, 53 Leninsky Prospekt, Moscow 119991, Russia*

[2]*All-Russia Research Institute of Automatics, 22 Sushchevskaya Street, Moscow 127055, Russia*

[3]*National Research Nuclear University MEPhI, 31 Kashirskoye Shosse, Moscow 115409, Russia*

[4]*Yanka Kupala State University of Grodno, 22 Ozheshko Street, Grodno 230023, Belarus*

(Received 4 December 2014; revised manuscript received 22 January 2015; published 27 February 2015)

We have investigated theoretically the spontaneous decay rate of an excited molecule placed near a circular aperture in a perfectly conducting infinitely thin plane screen. A quasistatic analytical solution for a molecule with an arbitrary position near the aperture is found. In a case with a retardation, an exact analytical solution expressed through spheroidal wave functions is obtained. Analytical results are in good agreement with numerical simulations. The results may be useful in the design and development of optical nanodevices based on the control of elementary quantum systems emission.

DOI: 10.1103/PhysRevA.91.023834 PACS number(s): 42.50.Ct, 68.37.Uv, 42.50.−p, 33.50.−j

## I. INTRODUCTION

A hole is a fundamental geometry in many areas because it concentrates any flows incident on it. Nowadays, different kinds of scanning microscopes where an aperture is the main part are basic tools for research of individual molecules [1–8] [see Fig. 1(a) for a schematic of the operation principle of a scanning near-field optical microscope]. Another important application of nanoholes is the development of sensitive detectors, sensors, and devices based on extraordinary light transmission through nanoholes [9–13] [see the schematic of such devices in Fig. 1(b)].

In these and other similar cases, the role of the hole in the system is to localize the energy of the electromagnetic field, allowing the effective interaction of light with single molecules placed inside or near the aperture.

Despite the wide use of holes in such devices, the interpretation of experimental data has not been a simple task until now. The structure of the electromagnetic field near the hole is complicated since the film in which a hole is perforated divides the space into two parts, i.e., the topology of the problem is significantly different from the topology of the scattering problem for a finite-volume particle. It is a fact that there is no simple model describing the field near the hole, whereas there are a number of relatively simple solutions for finite-size particles [14].

The impact of a hole on the radiation of a molecule is dual. On one hand, the hole modifies the electromagnetic field of the excitation field, and on the other hand, it modifies the rate of spontaneous emission of the molecule (the Purcell effect [15]). In this paper, we consider the problem of the modification of the spontaneous emission rate of a molecule placed near a circular hole in an infinitely thin and perfectly conducting [perfect electric conductor (PEC)] plane screen. A detailed description of the fluorescence of a molecule near a nanoaperture will be presented in a separate paper [16]. Throughout the paper, we will approximate the molecule radiation with the help of an oscillating point electric (or magnetic) dipole. Figure 2 illustrates the geometry of the problem schematically.

In the case of weak interaction of the molecule with the aperture, the molecule spontaneous decay rate in vacuum near the opening can be calculated with the help of the solution of the classical problem of field diffraction from the oscillating dipole source (with an optical frequency $\omega_0$ and a dipole momentum $\mathbf{d}_0$) on the aperture. In this case, the spontaneous decay rate $\gamma$, which is proportional to the radiation power in the classical case, can be represented as [17–20]

$$\frac{\gamma}{\gamma_0} = \frac{3}{2}\mathrm{Im}\left\{\frac{\mathbf{d}_0\cdot\mathbf{E}(\mathbf{r}_0,\mathbf{r}_0,\omega_0)}{k_0^3|\mathbf{d}_0|^2}\right\} = 1+\frac{3}{2}\mathrm{Im}\left\{\frac{\mathbf{d}_0\cdot\mathbf{E}^{(1)}(\mathbf{r}_0,\mathbf{r}_0,\omega_0)}{k_0^3|\mathbf{d}_0|^2}\right\}, \quad (1)$$

where $\mathbf{E}(\mathbf{r},\mathbf{r}_0,\omega_0)$ is the total electric field of the dipole placed at $\mathbf{r}_0$ in the presence of a hole and $\mathbf{E}^{(1)}(\mathbf{r},\mathbf{r}_0,\omega_0)$ is its scattered part. Both $\mathbf{E}(\mathbf{r},\mathbf{r}_0,\omega_0)$ and $\mathbf{E}^{(1)}(\mathbf{r},\mathbf{r}_0,\omega_0)$ can be found by solving Maxwell's equations with a dipole source. $\gamma_0 = (4k_0^3/3\hbar)|\mathbf{d}_0|^2$ stands for the rate of spontaneous emission in vacuum, $k_0 = \omega_0/c_0$, $c_0$ is the speed of light in vacuum, and Im describes the imaginary part.

Equation (1) describes the total rate of emission, i.e., it takes into account both processes of emitted photon absorption by the scattering body and pure radiative processes in which photons fly to infinity.

The radiative part of the spontaneous emission rate can be expressed in terms of the energy flux at infinity [17],

$$\frac{\gamma}{\gamma_0} = \frac{3}{8\pi k_0^4|\mathbf{d}_0|^2}\mathrm{Re}\left\{\int_S dS\big(\mathbf{E}(\mathbf{r},\mathbf{r}_0,\omega_0)\times\mathbf{H}^*(\mathbf{r},\mathbf{r}_0,\omega_0)\big)\cdot\mathbf{n}\right\}, \quad (2)$$

where $S$ is an infinitely distant closed surface, $\mathbf{n}$ is the outward normal to the surface, $\mathbf{E}(\mathbf{r},\mathbf{r}_0,\omega_0)$ and $\mathbf{H}(\mathbf{r},\mathbf{r}_0,\omega_0)$ are the electric and magnetic fields at the observation point $\mathbf{r}$, the asterisk denotes the complex conjugation, and Re describes the real part. In the case of a screen without losses, the total decay rate (1) and the rate of radiation (2) coincide. We will

*vklim@sci.lebedev.ru

 

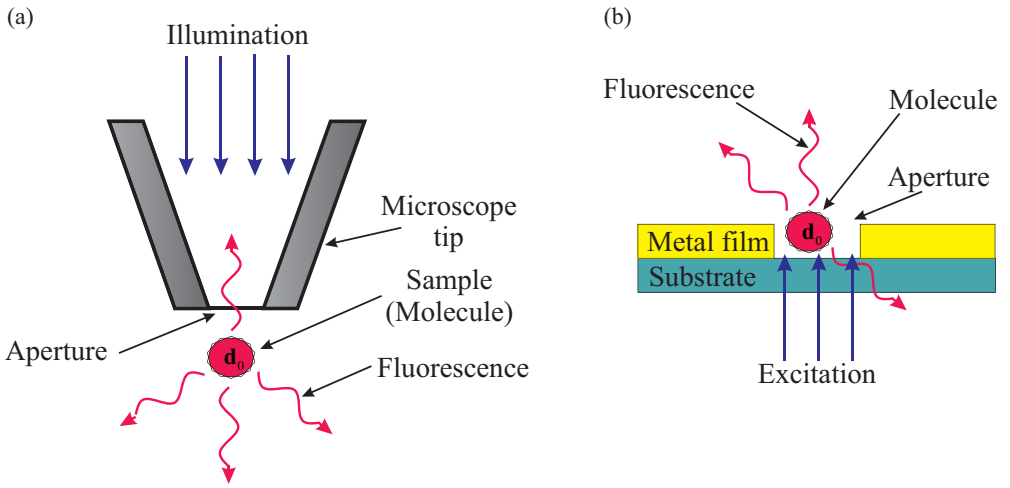


FIG. 1. (Color online) (a) A schematic of a scanning optical microscope and (b) a schematic of a plasmon biosensor based on a nanoaperture.

use both Eqs. (1) and (2) to check the calculation's correctness because in the case of a PEC screen there are no losses.

The rest of the paper is organized as follows. Section II provides an analytical solution for an arbitrary position of a molecule with an arbitrary orientation of the dipole momentum near an aperture of the radius $a$ within the quasistatic approximation ($r_0, a \ll \lambda_0$, where $\lambda_0$ is the wavelength of the molecule radiation in vacuum). Section III presents an analytical solution of Maxwell's equations by taking into account retardation effects in the case of a molecule located on the symmetry axis of the aperture with an arbitrary orientation of the dipole momentum. Section IV describes a numerical simulation of molecule radiation near a nanoaperture within the finite element method (COMSOL MULTIPHYSICS®). In Sec. V, we compare results obtained within numerical and analytical approaches.

## II. QUASISTATIC APPROXIMATION

Now, in most important applications of nanophotonics, the size of a hole is much smaller than the wavelength ($a \ll \lambda_0$), and a quasistatic approach where retardation effects can be neglected can be considered as a good approximation. In this special case, the analytical solution of the problem of spontaneous emission of a molecule near the nanohole can be found (see also Ref. [21]). The quasistatic solution is important

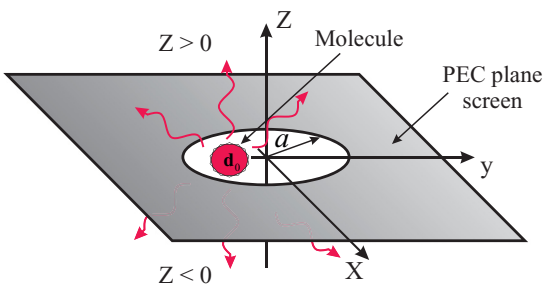


FIG. 2. (Color online) Geometry of the problem: An oscillating dipole with a dipole momentum $\mathbf{d}_0$ located near the nanoaperture of the radius $a$ in an infinitely thin PEC plane screen situated at $z = 0$.

both by itself and for checking of accuracy of calculations performed by other methods (see Secs. III and IV).

To find the solution of dipole radiation near a circular nanoaperture, we have used a toroidal coordinate system. Cartesian coordinates $(x, y, z)$ are related to the toroidal $(\eta, \xi, \varphi)$ $(0 \leqslant \eta < \infty, 0 \leqslant \xi \leqslant 2\pi, 0 \leqslant \varphi \leqslant 2\pi)$ through the following relations [22]:

$$x = a\frac{\sinh\eta}{\cosh\eta - \cos\xi}\cos\varphi, \quad y = a\frac{\sinh\eta}{\cosh\eta - \cos\xi}\sin\varphi,$$
$$z = a\frac{\sin\xi}{\cosh\eta - \cos\xi}. \tag{3}$$

Within these coordinates, the hole coincides with the coordinate surface, allowing an analytical solution of the boundary condition $E_{\tan} = 0$ on the perforated screen surface.

The expression for the potential of point charge near a circular nanoaperture of radius $a$ in a toroidal coordinate system is known [21,23] and has the following form (the coordinates of the source have subscript "0"):

$$\varphi_{\text{point charge}}(\mathbf{r},\mathbf{r}_0) = \frac{\sqrt{(\cosh\eta - \cos\xi)(\cosh\eta_0 - \cos\xi_0)}}{\pi a\sqrt{2}} \times \left[\frac{\frac{\pi}{2} + \arcsin\left(\frac{\cos[(\xi-\xi_0)/2]}{\cosh(\Omega/2)}\right)}{\sqrt{\cosh\ \Omega - \cos(\xi - \xi_0)}} - \frac{\frac{\pi}{2} + \arcsin\left(\frac{\cos[(\xi+\xi_0)/2]}{\cosh(\Omega/2)}\right)}{\sqrt{\cosh\ \Omega - \cos(\xi + \xi_0)}}\right], \tag{4}$$

where $\cosh\ \Omega = \cosh\eta\cosh\eta_0 - \sinh\eta\sinh\eta_0\cos(\varphi - \varphi_0)$. The potential $\varphi_{\text{dipole}}(\mathbf{r},\mathbf{r}_0)$ of the dipole source with charge density $\rho_{\text{dipole}} = (\mathbf{d}_0 \cdot \nabla_0)\delta^{(3)}(\mathbf{r} - \mathbf{r}_0)e^{-i\omega_0 t}$ can be found from Eq. (4) by differentiation,

$$\varphi_{\text{dipole}}(\mathbf{r},\mathbf{r}_0) = (\mathbf{d}_0 \cdot \nabla_0)\varphi_{\text{point charge}}(\mathbf{r},\mathbf{r}_0). \tag{5}$$

To describe the far-field radiation Eq. (2), one should find the expressions for the potential at long distances $r = \sqrt{x^2 + y^2 + z^2}$ from the nanoaperture. The corresponding

asymptotic expressions of Eq. (5) are

$$\varphi_{\text{dipole}}(\mathbf{r},\mathbf{r}_0) \approx \begin{cases} \dfrac{az}{\pi\sqrt{2}r^3}(\mathbf{d}_0\cdot\nabla_0)f^{(+)}(\xi_0,\eta_0) = \dfrac{zd^{(+)}_{\text{tot},z}}{r^3}, & z>0 \\ \dfrac{az}{\pi\sqrt{2}r^3}(\mathbf{d}_0\cdot\nabla_0)f^{(-)}(\xi_0,\eta_0) = \dfrac{zd^{(-)}_{\text{tot},z}}{r^3}, & z<0 \end{cases} \tag{6}$$

where the function $f^{(\pm)}(\xi,\eta)$ has the form

$$f^{(\pm)}(\xi,\eta) = \pm\frac{4\sin(\xi/2)}{\sqrt{\cosh\eta-\cos\xi}} + \frac{2\sqrt{2}\sin(\xi)\{\pi/2 \pm \arcsin[\cos(\xi/2)/\cosh(\eta/2)]\}}{\cosh\eta-\cos\xi}. \tag{7}$$

Expression (6) demonstrates that the potential has a dipolar character in both upper and lower half-spaces with only the dipole-moment $z$ component being nonzero. From Eq. (6), one can easily find the expressions for the dipole moments responsible for the emission into the upper $d^{(+)}_{\text{tot},z}$ and lower $d^{(-)}_{\text{tot},z}$ half-spaces, respectively,

$$d^{(\pm)}_{\text{tot},z} = \frac{a}{\pi\sqrt{2}}(\mathbf{d}_0\cdot\nabla)f^{(\pm)}(\xi,\eta)\Big|_{\substack{\xi=\xi_0,\\ \eta=\eta_0}} = \frac{(\cosh\eta-\cos\xi)}{\pi\sqrt{2}}\left(d_{0,\xi}\frac{\partial}{\partial\xi}+d_{0,\eta}\frac{\partial}{\partial\eta}\right)f^{(\pm)}(\xi,\eta)\Big|_{\substack{\xi=\xi_0,\\ \eta=\eta_0}}. \tag{8}$$

It is interesting that the resulting expression does not depend on the angular coordinate $\varphi$.

The dipolar character of the fields in both upper and lower half-spaces Eq. (6) allows us to calculate energy flows in both half-spaces easily. The total decay rate can be calculated as a sum of decay rates in the corresponding half-space. As a result, within the quasistatic approximation, we have obtained the following expression for the spontaneous emission rate of a molecule placed at the point $(\xi_0,\eta_0)$:

$$\frac{\gamma}{\gamma_0} = \left(\frac{\gamma}{\gamma_0}\right)^{(+)} + \left(\frac{\gamma}{\gamma_0}\right)^{(-)} = \frac{1}{2}\left(\frac{d^{(+)}_{\text{tot},z}}{|\mathbf{d}_0|}\right)^2 + \frac{1}{2}\left(\frac{d^{(-)}_{\text{tot},z}}{|\mathbf{d}_0|}\right)^2. \tag{9}$$

In Eq. (9), the first term ("+") describes the emission into the upper half-space ($z>0$), which is characterized by a dipole momentum $d^{(+)}_{\text{tot},z}$. The second term ("–") corresponds to radiation into the lower half-space ($z<0$), which is characterized by a dipole momentum $d^{(-)}_{\text{tot},z}$. It is interesting to note that regardless of the orientation of the dipole momentum $\mathbf{d}_0$, far-field radiation in the upper and lower half-spaces is determined by the effective electric dipole, which has only the $z$ orientation! Values of the dipole momenta of the upper and lower half-spaces are not equal ($d^{(+)}_{\text{tot},z} \neq d^{(-)}_{\text{tot},z}$). Thus, the radiation of the whole system does not have a true dipole character, despite an arbitrarily small size of the holes!

An important feature of this approach is the fact that in the case of $\varphi$ orientation of the molecule dipole momentum, the spontaneous emission is significantly suppressed at any position of the molecule and can be described by terms on the order of $(k_0a)^2$. It corresponds to magnetic dipole and quadrupole radiation and is of a higher order of smallness compared with Eq. (9).

Thus, within the quasistatic approximation the spontaneous emission of a molecule located near the nanoaperture can be described by relatively simple analytical Eq. (9) containing only elementary functions.

In special cases, Eq. (9) become very simple. For example, in the case of a molecule located on the symmetry axis ($z$ axis) at $z=z_0$ the radiation is only possible for the dipole momentum oriented along the $z$ axis. In this case, the total dipole momenta describing the radiation into the upper and lower half-spaces are of the form

$$\frac{d^{(\pm)}_{\text{tot},z}}{|\mathbf{d}_0|} = 1 \pm \frac{2}{\pi}\left[\frac{az_0}{a^2+z_0^2} + \arctan\left(\frac{z_0}{a}\right)\right] \quad (z \text{ orientation}). \tag{10}$$

When the molecule is situated at the center of the aperture $z_0=0$, we obtain $d^{(+)}_{\text{tot},z}/|\mathbf{d}_0| = d^{(-)}_{\text{tot},z}/|\mathbf{d}_0| = 1$, that is for a molecule in the center of the hole it emits as it radiates in free space. It is an expected result because for such a position a molecule does not feel the aperture due to the symmetry of its electric and magnetic fields. When $z_0 \gg a$, we have $d^{(+)}_{\text{tot},z}/|\mathbf{d}_0| = 2$, $d^{(-)}_{\text{tot},z}/|\mathbf{d}_0| = 0$, and the system radiates with a double dipole momentum into the upper half-space. Note that within the limit of the quasistatic approximation, the condition $z_0 \gg a$ means only $\lambda_0 \gg z_0 \gg a$ .

Now, let us consider the decay rate for a molecule with the $z$ orientation of the dipole momentum and situated in the plane of the screen $z=0$. In this situation, the decay rate of the molecule inside the hole does not change in comparison with the case of free space at any position $d^{(+)}_{\text{tot},z}/|\mathbf{d}_0| = d^{(-)}_{\text{tot},z}/|\mathbf{d}_0| = 1$. For a molecule located near the screen plane ($z_0 \to +0$), the dipole momenta describing the emission into the upper and lower half-spaces look like

$$\frac{d^{(\pm)}_{\text{tot},z}}{|\mathbf{d}_0|} = \begin{cases} 1, & \rho_0 \leqslant a \\ 1 \pm \dfrac{2}{\pi}\left[\dfrac{a}{\sqrt{\rho_0^2-a^2}} + \arcsin\left(\dfrac{\sqrt{\rho_0^2-a^2}}{\rho_0}\right)\right], & \rho_0 > a \end{cases} \quad (z \text{ orientation}), \tag{11}$$

where $\rho_0 = \sqrt{x_0^2+y_0^2}$.

From Eq. (11), one can see that near the rim of the hole there is a significant (infinite) enhancement of the decay rate, and the molecule radiates both in the upper and in the lower half-spaces. When taking into account finite thickness of the

screen and its finite permittivity, the spontaneous decay rate of a molecule near the rim of the hole becomes finite.

In the case of a molecule with $x$ orientation of the dipole momentum and placed in the plane $z = 0$, from Eqs. (7) and (8) one can easily find that the dipole momenta describing the fields in the upper and lower half-spaces will have the form

$$\frac{d^{(\pm)}_{\mathrm{tot},z}}{|\mathbf{d}_0|} = \begin{cases} \mp\dfrac{2}{\pi}\dfrac{\rho_0}{\sqrt{a^2-\rho_0^2}}\cos\varphi, & \rho_0 < a \\ 0, & \rho_0 \geqslant a \end{cases} \quad (x \text{ orientation}). \tag{12}$$

Outside the hole $\rho_0 \geqslant a$, the total dipole momentum is equal to zero due to the PEC boundary conditions. From Eq. (12), one can see that near the rim of the aperture, there is a significant (infinite) enhancement of the decay rate and the radiation propagates both into the upper and into the lower half-spaces. Taking into account the finite thickness of the screen and its finite permittivity, the spontaneous decay rate near the rim of the hole becomes limited again. For the $y$-oriented dipole momentum in the plane $z = 0$, there is a similar expression. The difference is in the angular dependence (in the $x$-orientation case, there is the $\cos\varphi$ factor, whereas in the $y$-orientation case there is the $\sin\varphi$ factor).

If the molecule is situated far from the aperture ($z_0 \gg \lambda_0$), the nanoaperture ceases to affect the emission, and one should use the expression for the spontaneous decay rate in the presence of a PEC plane screen without holes [18,19],

$$\frac{\gamma}{\gamma_0} = 1 - 3\left(\frac{\cos x}{x^2} - \frac{\sin x}{x^3}\right)\Big|_{x=2k_0z_0} \quad \text{(for the vertical dipole)}, \tag{13}$$

$$\frac{\gamma}{\gamma_0} = 1 - \frac{3}{2}\left(\frac{\sin x}{x} + \frac{\cos x}{x^2} - \frac{\sin x}{x^3}\right)\Big|_{x=2k_0z_0} \quad \text{(for the horizontal dipole)}. \tag{14}$$

Thus, the above-presented analytical expressions allow one to relatively easily estimate the spontaneous decay rate of a molecule (or other quantum emitter) placed near the nanoaperture with small losses and to interpret results of the single molecule observations with the help of near-field scanning microscopes.

## III. RETARDATION EFFECTS

Expressions of Sec. II are valid in the limit of a small hole only ($a, z_0 \ll \lambda_0$) where one can neglect retardation effects. For finite-size apertures, it is important to understand the significance of retardation effects. Therefore, in this section we present an exact solution for diffraction of an oscillating electric dipole field on a hole in a PEC plane screen.

Let us consider a molecule with an electric dipole momentum $\mathbf{d}_0$ located on the positive part of the Cartesian $z$ axis at a distance $z_0 > 0$ from a circular aperture of the radius $a$ in a PEC infinitely thin screen (situated at $z = 0$, see Fig. 2).

To solve this problem, we have used an oblate spheroidal coordinates system [24] in which, as is known, variables in the Helmholtz equation can be separated [25]. A solution of Maxwell's equations in this coordinate system can be built by a standard but tedious way of expansion of the solution over spheroidal functions and determination of unknown expansion coefficients from PEC boundary conditions at the perforated screen surface. For brevity, we will omit long algebraic calculations here and present only final expressions.

To calculate the spontaneous decay rate of a molecule, we use the definition (2); in doing so, we need an asymptotic behavior of the field at long distances from the origin. On the basis of Babinet's principle [26,27] and according to Refs. [28–31], we have found an exact expression for the transversal ($\theta$ and $\varphi$) component of the far fields in a spherical coordinate system $(r, \theta, \varphi)$ [$0 \leqslant r < \infty, 0 \leqslant \theta \leqslant \pi, 0 \leqslant \varphi < 2\pi$, the polar axis of the spherical coordinate system coincides with the symmetry axis of the hole (see Fig. 2)]. These components define energy flow to infinity and decrease with the distance as $\sim 1/r$, where $r = \sqrt{x^2+y^2+z^2}$.

In the case of the $z$ orientation of the dipole momentum ($\mathbf{d}_0 \,||\, z$), the asymptotic behavior of fields in the upper ($z > 0$) and lower ($z < 0$) half-spaces can be described by the following expressions:

$$E^{(+)}_\theta = H^{(+)}_\varphi = -k_0^2 d_{0,z}\frac{e^{ik_0r}}{r}\sum_{n=1,3,5,\ldots}^{\infty}\left(C_n\frac{\partial P_n(\cos\theta)}{\partial\theta} + D_n S^{(1)}_{1n}(-ik_0a,\cos\theta)\right), \qquad E^{(+)}_\varphi = H^{(+)}_\theta = 0, \tag{15}$$

and

$$E^{(-)}_\theta = H^{(-)}_\varphi = k_0^2 d_{0,z}\frac{e^{ik_0r}}{r}\sum_{n=1,3,5,\ldots}^{\infty} D_n S^{(1)}_{1n}(-ik_0a,\cos\theta), \qquad E^{(-)}_\varphi = H^{(-)}_\theta = 0, \tag{16}$$

respectively.

The coefficients $C_n$ and $D_n$ in Eqs. (15) and (16) are of the form

$$C_n = 2i^{n+1}(2n+1)\frac{\psi_n(k_0z_0)}{(k_0z_0)^2}, \qquad D_n = \frac{4i^{n+1}\sigma_{1n}(-ik_0a)R^{(1)}_{1n}(-ik_0a,i0)}{k_0\sqrt{z_0^2+a^2}N_{1n}(-ik_0a)R^{(3)}_{1n}(-ik_0a,i0)}R^{(3)}_{1n}\left(-ik_0a, i\frac{z_0}{a}\right), \tag{17}$$

where $\psi_n(k_0z_0) = (\pi k_0z_0/2)^{1/2}J_{n+1/2}(k_0z_0)$, $J_{n+1/2}(k_0z_0)$ is the Bessel function [30], and ($m = 0,1,2,\ldots,n$).

$$N_{mn}(-ik_0a) = \int_{-1}^{1} d\xi\left[S^{(1)}_{mn}(-ik_0a,\xi)\right]^2, \quad \sigma_{mn}(-ik_0a) = \lim_{\xi\to1}\frac{S^{(1)}_{mn}(-ik_0a,\xi)}{(1-\xi^2)^{m/2}}. \tag{18}$$

In Eqs. (15)–(18) and below, $S_{mn}^{(1)}(-ik_0a,\cos\theta)$ are the angular spheroidal functions of the first kind, and $R_{mn}^{(j)}(-ik_0a,iz_0/a)$ are the radial spheroidal functions of the $j$th kind ($j = 1,3$) [30]; $P_n^m(\cos\theta)$ stands for the associated Legendre function [$P_n(\cos\theta) = P_n^0(\cos\theta)$] [30].

In the case of the tangential orientation of the dipole momentum ($\mathbf{d}_0 \,||\, x$) for the asymptotic fields in the upper ($z > 0$) and lower ($z < 0$) half-spaces we have the following expressions:

$$E_\theta^{(+)} = H_\varphi^{(+)} = -k_0^2 d_{0,x}\frac{e^{ik_0r}}{r}\sum_{n=1,3,5,\ldots}^{\infty}\left[F_{n+1}\frac{\partial P_{n+1}^1(\cos\theta)}{\partial\theta} - G_n\frac{P_n^1(\cos\theta)}{\sin\theta}\right.$$
$$\left. - A_n S_{0n}^{(1)}(-ik_0a,\cos\theta)\cos\theta + B_n S_{1n}^{(1)}(-ik_0a,\cos\theta)\sin\theta\right]\cos\varphi,$$
$$E_\varphi^{(+)} = -H_\theta^{(+)} = k_0^2 d_{0,x}\frac{e^{ik_0r}}{r}\sum_{n=1,3,5,\ldots}^{\infty}\left[F_{n+1}\frac{P_{n+1}^1(\cos\theta)}{\sin\theta} - G_n\frac{\partial P_n^1(\cos\theta)}{\partial\theta} - A_n S_{0n}^{(1)}(-ik_0a,\cos\theta)\right]\sin\varphi, \tag{19}$$

and

$$E_\theta^{(-)} = H_\varphi^{(-)} = -k_0^2 d_{0,x}\frac{e^{ik_0r}}{r}\sum_{n=1,3,5,\ldots}^{\infty}\left[A_n S_{0n}^{(1)}(-ik_0a,\cos\theta)\cos\theta - B_n S_{1n}^{(1)}(-ik_0a,\cos\theta)\sin\theta\right]\cos\varphi,$$
$$E_\varphi^{(-)} = -H_\theta^{(-)} = k_0^2 d_{0,x}\frac{e^{ik_0r}}{r}\sum_{n=1,3,5,\ldots}^{\infty}A_n S_{0n}^{(1)}(-ik_0a,\cos\theta)\sin\varphi, \tag{20}$$

respectively.

In Eqs. (19) and (20), the coefficients are of the form

$$F_{n+1} = -2i^n\frac{2n+3}{(n+1)(n+2)}\frac{1}{k_0z_0}\frac{d}{dx}\psi_{n+1}(x)\Big|_{x=k_0z_0}, \qquad G_n = 2i^{n+1}\frac{2n+1}{n(n+1)}\frac{\psi_n(k_0z_0)}{k_0z_0},$$
$$A_n = \frac{2i^n S_{0n}^{(1)}(-ik_0a,1)R_{0n}^{(1)'}(-ik_0a,i0)}{N_{0n}(-ik_0a)R_{0n}^{(3)'}(-ik_0a,i0)}R_{0n}^{(3)}\left(-ik_0a,i\frac{z_0}{a}\right) + \frac{2i^{n+1}Cd_1^{0n}(-ik_0a)}{k_0aN_{0n}(-ik_0a)R_{0n}^{(3)'}(-ik_0a,i0)}, \tag{21}$$
$$B_n = \frac{4i^{n+1}Cd_0^{1n}(-ik_0a)}{k_0aN_{1n}(-ik_0a)R_{1n}^{(3)}(-ik_0a,i0)},$$

where $(-1)^m d_r^{mn}(-ik_0a)$ is the expansion coefficient of the angular spheroidal function in a series of associated Legendre functions [24,29],

$$C = \frac{1}{T}\sum_{n=1,3,5,\ldots}^{\infty}\frac{S_{0n}^{(1)}(-ik_0a,1)S_{0n}^{(1)'}(-ik_0a,0)}{N_{0n}(-ik_0a)R_{0n}^{(3)'}(-ik_0a,i0)}R_{0n}^{(3)}\left(-ik_0a,i\frac{z_0}{a}\right),$$
$$T = \sum_{n=1,3,5,\ldots}^{\infty}\left\{\frac{d_1^{0n}(-ik_0a)S_{0n}^{(1)'}(-ik_0a,0)R_{0n}^{(3)}(-ik_0a,i0)}{N_{0n}(-ik_0a)R_{0n}^{(3)'}(-ik_0a,i0)} - \frac{2d_0^{1n}(-ik_0a)S_{1n}^{(1)}(-ik_0a,0)R_{1n}^{(3)'}(-ik_0a,i0)}{N_{1n}(-ik_0a)R_{1n}^{(3)}(-ik_0a,i0)}\right\}, \tag{22}$$

and where ($j = 1,3$)

$$R_{mn}^{(j)'}(-ik_0a,i\eta_0) = \frac{d}{d\eta}R_{mn}^{(j)}(-ik_0a,i\eta)\Big|_{\eta=\eta_0}, \qquad S_{mn}^{(1)'}(-ik_0a,\xi_0) = \frac{d}{d\xi}S_{mn}^{(1)}(-ik_0a,\xi)\Big|_{\xi=\xi_0}. \tag{23}$$

If $z_0 = 0$ for the coefficients $A_n$ and $B_n$, we have expressions [29],

$$A_n|_{z_0=0} = -\frac{2i^{n+1}S_{0n}^{(1)}(-ik_0a,1)}{k_0aN_{0n}(-ik_0a)R_{0n}^{(3)'}(-ik_0a,i0)} + \frac{2i^{n+1}Dd_1^{0n}(-ik_0a)}{(k_0a)^3N_{0n}(-ik_0a)R_{0n}^{(3)'}(-ik_0a,i0)},$$
$$B_n|_{z_0=0} = \frac{4i^{n+1}Dd_0^{1n}(-ik_0a)}{(k_0a)^3N_{1n}(-ik_0a)R_{1n}^{(3)}(-ik_0a,i0)}, \tag{24}$$

where

$$D = \frac{1}{L}\sum_{n=1,3,5,\ldots}^{\infty} i^n \frac{d_1^{0n}(-ik_0a)S_{0n}^{(1)}(-ik_0a,1)}{N_{0n}(-ik_0a)R_{0n}^{(3)'}(-ik_0a,i0)},$$

$$L = \sum_{n=1,3,5,\ldots}^{\infty}\left\{ i^n \frac{S_{0n}^{(1)}(-ik_0a,1)S_{0n}^{(1)'}(-ik_0a,1)}{N_{0n}(-ik_0a)R_{0n}^{(3)'}(-ik_0a,i0)} + \frac{2Md_0^{1n}(-ik_0a)\sigma_{1n}(-ik_0a)R_{1n}^{(3)'}(-ik_0a,i0)}{N_{1n}(-ik_0a)R_{1n}^{(3)}(-ik_0a,i0)} \right.$$
$$\left. - \frac{Md_1^{0n}(-ik_0a)\left[S_{0n}^{(1)'}(-ik_0a,1) - (k_0a)^2 S_{0n}^{(1)}(-ik_0a,1)\right]R_{0n}^{(3)}(-ik_0a,i0)}{N_{0n}(-ik_0a)R_{0n}^{(3)'}(-ik_0a,i0)} \right\},$$

$$M = \frac{1}{T}\sum_{n=1,3,5,\ldots}^{\infty} i^n \frac{S_{0n}^{(1)}(-ik_0a,1)S_{0n}^{(1)'}(-ik_0a,0)}{N_{0n}(-ik_0a)R_{0n}^{(3)'}(-ik_0a,i0)}. \tag{25}$$

Knowing the fields in the upper and lower half-spaces, it is possible to calculate the spontaneous emission rate by the formula,

$$\frac{\gamma}{\gamma_0} = \left(\frac{\gamma}{\gamma_0}\right)^{(+)} + \left(\frac{\gamma}{\gamma_0}\right)^{(-)}, \tag{26}$$

where

$$\left(\frac{\gamma}{\gamma_0}\right)^{(+)} = \frac{3}{8\pi k_0^4|\mathbf{d}_0|^2}\int_0^{\pi/2} d\theta \sin\theta \int_0^{2\pi} d\varphi\, r^2\left(\left|E_\theta^{(+)}\right|^2 + \left|E_\varphi^{(+)}\right|^2\right),$$
$$\left(\frac{\gamma}{\gamma_0}\right)^{(-)} = \frac{3}{8\pi k_0^4|\mathbf{d}_0|^2}\int_{\pi/2}^{\pi} d\theta \sin\theta \int_0^{2\pi} d\varphi\, r^2\left(\left|E_\theta^{(-)}\right|^2 + \left|E_\varphi^{(-)}\right|^2\right) \tag{27}$$

are the spontaneous decay rates of a molecule in the upper and lower half-spaces, respectively.

Using these expressions, we can find the asymptotic formula for the spontaneous decay rate in the case of the nanoaperture ($k_0a \to 0$) and for specific positions of the dipole near the aperture. These asymptotes should correspond to the quasistatic results of Sec. II.

### A. Dipole with vertical orientation ($\mathbf{d_0} \,||\, z$)

To find the long wavelength asymptote of Eq. (26) ($k_0z_0 \sim k_0a \ll 1$), one should take into account that the main contribution to the expression will be from the first terms in a series with the index $n = 1$. Using the following approximate expression [29,31]:

$$N_{11}(-ik_0a) \approx \frac{4}{3}, \qquad \sigma_{11}(-ik_0a) \approx 1, \qquad R_{11}^{(1)}(-ik_0a,i0) \approx \frac{k_0a}{3}, \qquad R_{11}^{(3)}(-ik_0a,i0) \approx \frac{k_0a}{3} - \frac{3i\pi}{4(k_0a)^2},$$
$$R_{11}^{(3)}\left(-ik_0a, i\frac{z_0}{a}\right) \approx \frac{1}{3}k_0\sqrt{z_0^2+a^2} - \frac{3i\pi\sqrt{z_0^2+a^2}}{4a(k_0a)^2}\left(1 - \frac{2z_0a}{\pi\left(z_0^2+a^2\right)} - \frac{2}{\pi}\arctan\frac{z_0}{a}\right), \tag{28}$$

from Eq. (28) we find for the coefficients (17),

$$C_1 \approx -2, \quad D_1 \approx -1 + \frac{2z_0a}{\pi\left(z_0^2+a^2\right)} + \frac{2}{\pi}\arctan\frac{z_0}{a}. \tag{29}$$

As a result, the asymptotic expressions for the fields Eqs. (15) and (16) take the form [$S_{11}^{(1)}(-ik_0a, \cos\theta) \approx \sin\theta$],

$$E_\theta^{(\pm)} = H_\varphi^{(\pm)} \approx -k_0^2 d_{0,z}\left[1 \pm \frac{2}{\pi}\left(\frac{z_0a}{z_0^2+a^2} + \arctan\frac{z_0}{a}\right)\right]\frac{e^{ik_0r}}{r}\sin\theta, \qquad E_\varphi^{(\pm)} = H_\theta^{(\pm)} = 0. \tag{30}$$

Substituting Eq. (30) into Eq. (27), we obtain the following expression for the decay rate in this approximation:

$$\left(\frac{\gamma}{\gamma_0}\right)^{(\pm)} \approx \frac{1}{2}\left[1 \pm \frac{2}{\pi}\left(\frac{z_0a}{z_0^2+a^2} + \arctan\frac{z_0}{a}\right)\right]^2, \tag{31}$$

which coincides with the result obtained in Sec. II within the quasistatic approximation [see Eqs. (9) and (10)] and confirms the correctness of the calculations in the retardation case.

### B. Dipole with a horizontal orientation ($\mathbf{d_0} \,||\, x$)

In the case of the horizontal dipole, it is very difficult to derive asymptotic expressions for the fields since the coefficients of Eqs. (22) and (25) are presented in the form

of a complicated series. Thus, to obtain satisfactory values, it is necessary to sum many terms of the series.

In what follows, we consider only the tangential dipole located on the plane of the aperture ($z_0 = 0$) . In this case, the main contribution to the asymptotic behavior of the fields Eqs. (19) and (20) will be determined by the terms with the index $n = 1$.

Our calculations show that a reasonably accurate value of the coefficient $D$ [see Eq. (25)] obtained by the summation of the series is of the form $D \approx -\frac{1}{3}(k_0 a)^2$. Using this expression, together with Eq. (28) and approximate expressions from [29]

$$N_{01}(-ik_0a) \approx \frac{2}{3}, \quad d_1^{01}(-ik_0a) \approx d_0^{11}(-ik_0a) \approx 1,$$
$$S_{01}^{(1)}(-ik_0a,1) \approx 1, \quad R_{01}^{(3)'}(-ik_0a,i0) \approx \frac{k_0a}{3} + \frac{3i\pi}{2(k_0a)^2}, \tag{32}$$

one can find asymptotic expressions for the coefficients (24) as follows:

$$A_1|_{z_0=0} \approx -i\frac{8k_0a}{3\pi}, \quad B_1|_{z_0=0} \approx i\frac{4k_0a}{3\pi}. \tag{33}$$

Substituting Eq. (33) into Eqs. (19) and (20), we find the asymptotic behavior of the fields [$F_2|_{z_0=0} = G_1|_{z_0=0} = 0$, $S_{01}^{(1)}(-ik_0a, \cos\theta) \approx \cos\theta$, $S_{11}^{(1)}(-ik_0a, \cos\theta) \approx \sin\theta$],

$$E_\theta^{(\pm)} = H_\varphi^{(\pm)} \approx \mp ik_0^2 d_{0,x}\frac{4k_0a}{3\pi}\frac{e^{ik_0r}}{r}(2-\sin^2\theta)\cos\varphi,$$
$$E_\varphi^{(\pm)} = -H_\theta^{(\pm)} \approx \pm ik_0^2 d_{0,x}\frac{8k_0a}{3\pi}\frac{e^{ik_0r}}{r}\cos\theta\sin\varphi. \tag{34}$$

The resulting expressions (34) coincide with the expressions [28], that can be obtained from the fields' asymptotes of the problem of a magnetic dipole placed near a PEC plane disk [28] and Babinet's principle. Found expressions suggest that the horizontal dipole radiation on the plane of the aperture is not a pure dipole one. Substituting Eq. (34) into Eq. (27) and making use of Eq. (26), we find the asymptotic behavior (see also Ref. [14]),

$$\frac{\gamma}{\gamma_0} \approx \frac{64}{15\pi^2}(k_0a)^2. \tag{35}$$

Thus, this section presents analytical expressions for the spontaneous decay rate of the molecule located on the symmetry axis of the hole by taking into account the retardation effects. In the quasistatic limit, these expressions coincide with the results of Sec. II. This coincidence confirms the validity of the results of this section which take retardation effects into account.

## IV. NUMERICAL SIMULATION

A complete analytical solution of the problem of spontaneous emission of a molecule near the hole, presented in Sec. III, is based on the use of spheroidal functions. Calculation of these functions is still not an easy task. Therefore, this section provides a description of a numerical method for calculation of the molecule spontaneous emission rate. The method is based on the numerical solution of Maxwell's equations by the finite element method. We use a commercial realization of the finite element method in the software product COMSOL MULTIPHYSICS®.

The geometries of the numerical simulations are shown in Fig. 3. The geometry of Fig. 3(a) describes the direct solution for a radiating electric dipole, whereas the geometry of Fig. 3(b) describes the auxiliary problem of radiation of a magnetic dipole near the disk, which is used to find the spontaneous decay rate of an electric dipole near the hole using Babinet's principle [26].

An expression for the total spontaneous decay rate for the direct problem is described by the formula (1). In the case of the geometry of Fig. 3(b), the expression (1) can be rewritten with the help of Babinet's principle as

$$\frac{\gamma}{\gamma_0} = 1 + \frac{3}{2}\mathrm{Im}\left(\frac{\mathbf{d}_0 \cdot \mathbf{E}_{\mathrm{plate}}^{(1)}(\mathbf{r}_0,\mathbf{r}_0,\omega_0)}{k_0^3|\mathbf{d}_0|^2}\right)$$
$$+ \frac{3}{2}\mathrm{Im}\left(\frac{\mathbf{d}_0 \cdot \mathbf{H}_{\mathrm{disk}}^{(1)}(\mathbf{r}_0,\mathbf{r}_0,\omega_0)}{k_0^3|\mathbf{d}_0|^2}\right), \tag{36}$$

where $\mathbf{E}_{\mathrm{plate}}^{(1)}$ is the scattered field in the problem of the "electric dipole near the PEC plane without a hole," $\mathbf{H}_{\mathrm{disk}}^{(1)}$ is the scattered magnetic field in the problem of the "oscillating magnetic dipole with magnetic momentum $\mathbf{d}_0$ near the PEC disk."

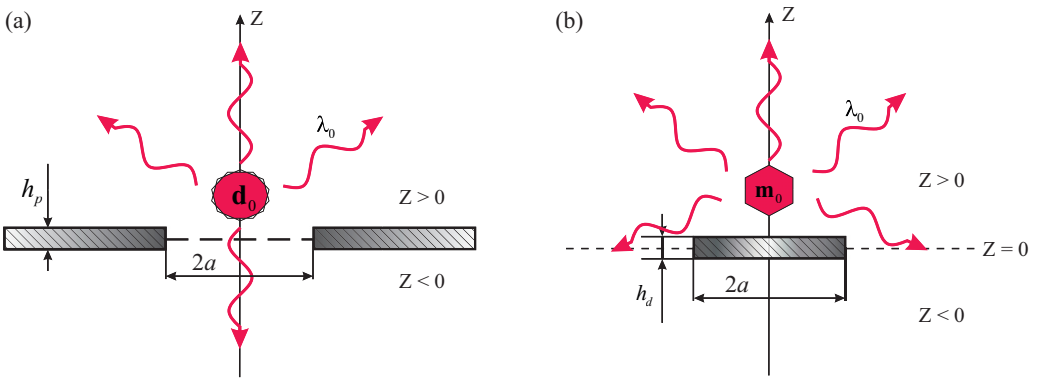


FIG. 3. (Color online) Schematic of the geometry of the numerical simulation. (a) An electric dipole with the dipole momentum $\mathbf{d}_0$ is located in vacuum on the symmetry axis of the hole in a PEC plane screen. The thickness of the screen is $h_p = 10$ nm. The aperture radius is $a$. (b) A magnetic dipole with the dipole momentum $\mathbf{m}_0 = \mathbf{d}_0$ is located in vacuum on the symmetry axis of a PEC plane disk with a thickness of $h_d = 10$ nm. The disk radius is $a$.

Taking into account the expression for the decay rate of the molecule near the PEC surface (13) and (14), we obtain

$$\frac{\gamma}{\gamma_0} = 1 - 3\left(\frac{\cos x}{x^2} - \frac{\sin x}{x^3}\right)\Big|_{x=2k_0z_0} + \frac{3}{2}\mathrm{Im}\left(\frac{\mathbf{d}_0 \cdot \mathbf{H}^{(1)}_{\mathrm{disk}}(\mathbf{r}_0,\mathbf{r}_0,\omega_0)}{k_0^3|\mathbf{d}_0|^2}\right) \quad (37)$$

for a vertical dipole and

$$\frac{\gamma}{\gamma_0} = 1 - \frac{3}{2}\left(\frac{\sin x}{x} + \frac{\cos x}{x^2} - \frac{\sin x}{x^3}\right)\Big|_{x=2k_0z_0} + \frac{3}{2}\mathrm{Im}\left(\frac{\mathbf{d}_0 \cdot \mathbf{H}^{(1)}_{\mathrm{disk}}(\mathbf{r}_0,\mathbf{r}_0,\omega_0)}{k_0^3|\mathbf{d}_0|^2}\right) \quad (38)$$

for a horizontal dipole.

Equations (37) and (38) have been used to find the spontaneous decay rate of a molecule near the hole based on the calculation of the problem of a magnetic dipole near a circular PEC plane disk. Additional calculations within the geometry Fig. 3(b) have been used to verify the numerical results within the geometry Fig. 3(a) as well as to improve them. When using the numerical finite element method, an infinitely thin PEC screen or a disk has been approximated by a screen or a disk of a finite thickness ($h_p = h_d = 10\,\mathrm{nm}$). As a result of such an approximation, the decay rate of the $z$-oriented dipole placed near the hole rim tends to zero, and it does not correspond to its behavior near the infinitely thin PEC screen. When considering the problem of the magnetic dipole near the disk, such a problem does not occur, and calculations become more accurate.

## V. ANALYSIS OF THE RESULTS AND GRAPHIC ILLUSTRATIONS

Let us now consider what the proposed approaches predict and how their results agree with each other. In Fig. 4, the spontaneous decay rates of a molecule with a vertical orientation of the dipole momentum and located on the symmetry axis of the system are shown as functions of distance from the center of the hole for different ratios of the radius $a$ and the wavelength $\lambda_0$.

From Fig. 4, it is clear that by moving the molecule from the center of the hole at a distance greater than $3a$, the effect of the hole becomes very small. In this case, for calculation of the spontaneous decay rate of the molecule the simple Eq. (13), describing the emission of a molecule near a PEC plane screen without holes, works well. If the distance is less than the radius $a$, the quasistatic approximation discussed in Sec. II describes the process well. For the description of the molecular emission in the intermediate interval from $a$ to $3a$, one should either use an exact calculation using spheroidal functions or carry out numerical simulations. With increasing of the wavelength for the fixed hole diameter, the combination of the quasistatic solution and the solution near the plane without the hole becomes more and more accurate. However, numerical modeling of an electric dipole near the aperture gives decay rates that are smaller than analytical results due to the finite thickness of the screen. Computations that make use of Babinet's principle are in good agreement with analytical results.

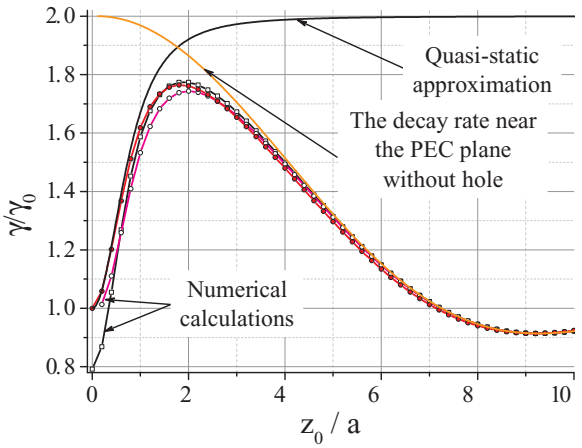


FIG. 4. (Color online) The decay rate $\gamma/\gamma_0$ of the molecule, located on the symmetry axis of the hole (the aperture radius is $a = 50\,\mathrm{nm}$; the wavelength is $\lambda_0 = 1000\,\mathrm{nm}$, $z$-oriented dipole). The solid black curve is a quasistatic approximation; the black curve with dots is a direct numerical calculation for the electric dipole; the magenta curve with dots is the numerical calculations using Babinet's principle; the red curve with dots is an analytical calculation; the orange curve is the decay rate near the PEC plane without holes.

Note that for any parameters of the hole, the molecule with a vertical dipole momentum located in the center of the hole does not feel the hole and its decay rate is equal to the decay rate in vacuum.

Analytical calculations for a molecule with a horizontal dipole momentum are much more difficult in this case, and expressions for decay rates beyond the quasistatic

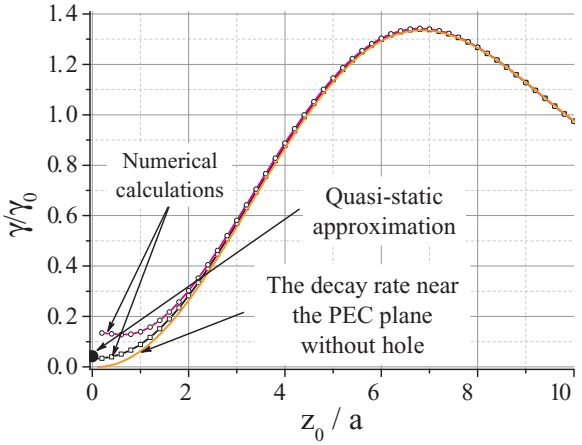


FIG. 5. (Color online) The decay rate $\gamma/\gamma_0$ of a molecule located on the symmetry axis of the aperture as a function of the distance $z_0$ to the aperture (the aperture radius is $a = 50\,\mathrm{nm}$; the wavelength is $\lambda_0 = 1000\,\mathrm{nm}$, horizontal dipole momentum). The big black point is a quasistatic approximation (35); the black curve with dots is a direct numerical calculation; the magenta curve with dots is the numerical calculations using Babinet's principle; the orange curve is the decay rate near the PEC plane without holes.

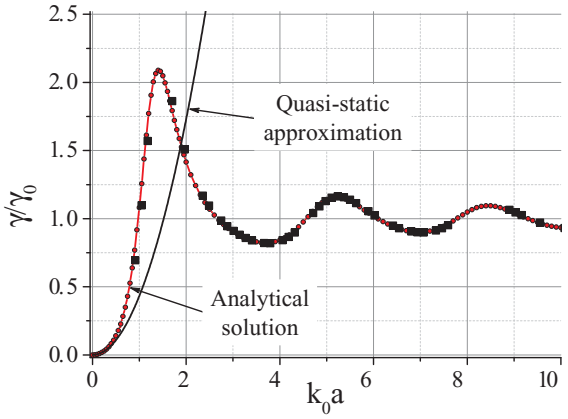


FIG. 6. (Color online) The decay rate $\gamma/\gamma_0$ of the molecule with a horizontal dipole momentum located in the center of the hole as a function of the hole radius $a$. The black curve is a quasistatic approximation, the red curve with dots is an analytical calculation, and the black squares are a numerical calculation.

approximation can be obtained only for a molecule located in the center of the hole.

Figure 5 show results of the calculation of the spontaneous decay rate of a molecule with a horizontal dipole momentum located on the symmetry axis of the hole as a function of the distance to the aperture center.

From Fig. 5, one can see that, as well as for a molecule with a vertical dipole moment, when moving a molecule with a horizontal dipole moment at a distance of more than $3a$, the hole influence becomes negligible and the system can be described well by the approach of "a molecule near a PEC plane without a hole."

Figure 6 shows the results of analytical and numerical calculations of the decay rate of a molecule with a horizontal dipole momentum, located in the center of the hole as a function of the aperture radius ($k_0a$).

From Fig. 6, one can see that the molecule with a horizontal dipole momentum situated in the center of the hole has a significant impact from the hole, and even a small hole ($k_0a \sim 1$) increases the decay rate by more than two times.

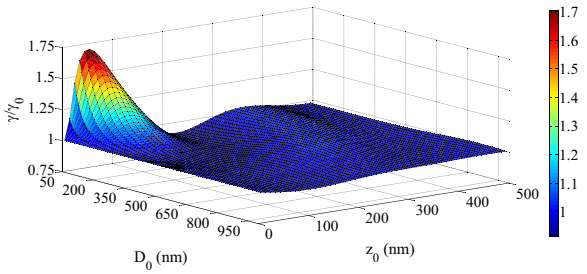


FIG. 7. (Color online) The decay rate $\gamma/\gamma_0$ of the molecule with vertical orientation of the electric dipole momentum and located on the axis of the aperture as a function of the coordinate $z_0$ and the hole diameter $D_0$. Babinet's principle has been used [see Eq. (37) and Fig. 3(b)]. The wavelength is $\lambda_0 = 500$ nm. The thickness of the complementary disk is $h_d = 10$ nm.

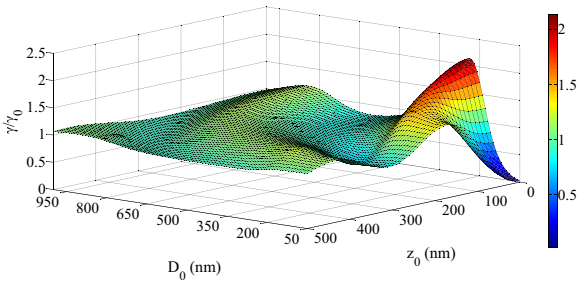


FIG. 8. (Color online) The decay rate $\gamma/\gamma_0$ of a molecule with horizontal orientation of the electric dipole momentum and located on the aperture axis as a function of the coordinate $z_0$ and the hole diameter $D_0$. The wavelength is $\lambda_0 = 500$ nm. The thickness of the screen is $h_p = 10$ nm.

Figure 6 also shows that the decay rate of the molecule placed in the center of the hole found by numerical methods is in good agreement with pure analytical calculations.

Below, we demonstrate the decay rate of the molecule as a function of its position on the axis and the diameter aperture $D_0 = 2a$. The wavelength $\lambda_0$ is equal to 500 nm.

In Fig. 7, one can see the case of a molecule with vertical orientation of the dipole momentum. Here, the decay rate has its maximum when the diameter is equal to 50–250 nm and the molecule is placed at a distance of ∼100 nm from the plate. The decay rate decreases monotonically as the aperture diameter increases. By increasing the diameter or the distance, the influence of the hole becomes small, and the decay rate goes to a value of 1 as in the case of vacuum.

Figure 8 shows the total decay rate of the molecule as a function of the hole diameter and the molecule position on the hole axis for the case of a horizontal orientation of the dipole momentum.

From Fig. 8, one can see that when the molecule is located near the center of a hole with a diameter of about 200 nm, the spontaneous decay rate has the maximum $\gamma/\gamma_0 \approx 2.1$, that is greater than for a plane without a hole (see also Fig. 6).

Until now, we have analyzed a molecule situated on the axis of symmetry. However, the most substantial enhancement of the decay rate one can observe is near the hole rim. This enhancement is due to the rim sharpness and can be described well by a quasistatic solution. In Figs. 9 and 10, the dependence

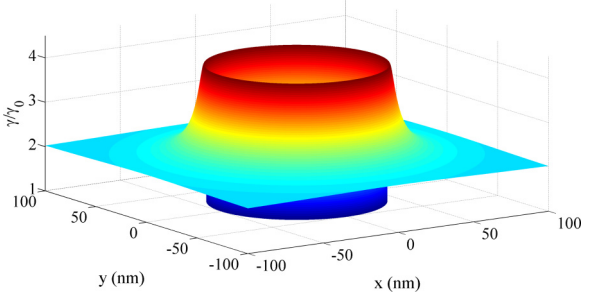


FIG. 9. (Color online) The decay rate of a molecule with the $z$-oriented dipole momentum as a function of the $x$ and $y$ coordinates on the plane $z = 5$ nm (quasistatic approximation). The hole diameter is 100 nm.

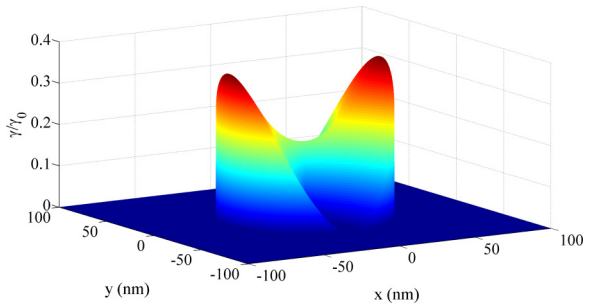


FIG. 10. (Color online) The decay rate of molecule with an $x$-oriented dipole momentum as a function of $x$ and $y$ coordinates on the plane $z = 5$ nm (quasistatic approximation). The diameter of the hole is 100 nm.

of decay rates of a molecule with different orientations are shown as a function of its position in the plane $z = 5$ nm.

From these figures, one can see that indeed near the hole rim the decay rates become very large due the rim sharpness. In real situations with smoothed hole rims, these infinites are reduced in value, but the general picture remains the same.

## VI. CONCLUSION

This paper presents a detailed theoretical analysis of the spontaneous emission of a molecule located near a circular hole in a PEC infinitely thin screen. We have found explicit analytical descriptions both within a quasistatic approximation and within a full system of Maxwell's equations by taking into account all retardation effects. Our analytical results give a clear picture of the spontaneous emission rate near nanoapertures and can be used both for testing numerical simulation algorithms for more complicated cases and for a fast preliminary analysis of experimental data.

In this study, we have examined the influence of the nanoaperture on the rate of spontaneous emission of molecules in its vicinity. However, the fluorescence of the molecules near the hole is determined not only by the spontaneous emission rate, but also by the excitation field intensity at the location of the molecule. Investigation of the molecule fluorescence taking into account both these factors will be presented in a separate paper [16] where it will be shown that the image of the molecule scanning microscope depends significantly not only on the orientation and position of the molecule, but also on the intensity of the excitation beam.

## ACKNOWLEDGMENTS

The research was supported by the Advanced Research Foundation (Contract No. 7/004/2013-2018). The authors are also grateful to the Belarusian Republican Foundation for Fundamental Research (Grant No. F12R-006, DG), the Russian Foundation for Basic Research (Grants No. 14-02-00290 and No. 15-52-52006), the Skolkovo Foundation, and the Russian Quantum Center for financial support of this work.

[1] *Near Field Optics*, edited by D. W. Pohl and D. Courjon (Kluwer Academic, Dordrecht, 1992).
[2] *Near Field Nano/Atom Optics and Technology*, edited by M. Ohtsu (Springer, Japan, 1998).
[3] J. P. Fillard, *Near Field Optics and Nanoscopy* (World Scientific, Singapore, 1998).
[4] *Nano-Optics*, edited by S. Kawata, M. Ohtsu, and M. Irie (Springer, Berlin, 2002).
[5] H. Gersen, M. F. García-Parajó, L. Novotny, J. A. Veerman, L. Kuipers, and N. F. van Hulst, Influencing the angular emission of a single molecule, Phys. Rev. Lett. **85**, 5312 (2000).
[6] H. Gersen, M. F. García-Parajó, L. Novotny, J. A. Veerman, L. Kuipers, and N. F. van Hulst, Near-field effects in single molecule emission, J. Microsc. **202**, 374 (2001).
[7] J. A. Veerman, M. F. Garcia-Parajo, L. Kuipers, and N. F. van Hulst, Single molecule mapping of the optical field distribution of probes for near-field microscopy, J. Microsc. **194**, 477 (1999).
[8] B. Sick, B. Hecht, U. P. Wild, and L. Novotny, Probing confined fields with single molecules and vice versa, J. Microsc. **202**, 365 (2001).
[9] H. Rigneault, J. Capoulade, J. Dintinger, J. Wenger, N. Bonod, E. Popov, T. W. Ebbesen, and P. F. Lenne, Enhancement of single-molecule fluorescence detection in subwavelength apertures, Phys. Rev. Lett. **95**, 117401 (2005).
[10] J. Wenger, D. Gérard, J. Dintinger, O. Mahboub, N. Bonod, E. Popov, T. W. Ebbesen, and H. Rigneault, Emission and excitation contributions to enhanced single molecule fluorescence by gold nanometric apertures, Opt. Express **16**, 3008 (2008).
[11] H. Aouani, O. Mahboub, E. Devaux, H. Rigneault, T. W. Ebbesen, and J. Wenger, Large molecular fluorescence enhancement by a nanoaperture with plasmonic corrugations, Opt. Express **19**, 13056 (2011).
[12] P.-F. Lenne, H. Rigneault, D. Marguet, and J. Wenger, Fluorescence fluctuations analysis in nanoapertures: Physical concepts and biological applications, Histochem. Cell Biol. **130**, 795 (2008).
[13] S. F. Heucke, F. Baumann, G. P. Acuna, P. M. D. Severin, S. W. Stahl, M. Strackharn, I. H. Stein, P. Altpeter, P. Tinnefeld, and H. E. Gaub, Placing individual molecules in the center of nanoapertures, Nano Lett. **14**, 391 (2014).
[14] V. V. Klimov, *Nanoplasmonics* (Pan Stanford, Singapore, 2014).
[15] E. Purcell, Spontaneous emission probabilities at radio frequencies, Phys. Rev. **69**, 681 (1946).
[16] V. V. Klimov, D. V. Guzatov, and I. V. Treshin, Fluorescence of a molecule placed near a circular aperture (unpublished).
[17] V. V. Klimov, M. Ducloy, and V. S. Letokhov, Spontaneous emission of an atom in the presence of nanobodies, Quantum Electron. **31**, 569 (2001).
[18] J. M. Wylie and J. E. Sipe, Quantum electrodynamics near interface, Phys. Rev. A **30**, 1185 (1984).
[19] J. M. Wylie and J. E. Sipe, Quantum electrodynamics near interface. II, Phys. Rev. A **32**, 2030 (1985).
[20] L. Novotny and B. Hecht, *Principles of Nano-Optics* (Cambridge University Press, New York, 2006).
[21] V. V. Klimov, Spontaneous emission of an atom placed near the aperture of a scanning microscope, JETP Lett. **78**, 471 (2003).

[22] P. Moon and D. E. Spencer, *Field Theory Handbook, Including Coordinate Systems, Differential Equations and Their Solutions*, 2nd ed. (Springer-Verlag, Berlin/Heidelberg/New York, 1971).

[23] H. Buchholz, *Elektrische und Magnetische Potentialfelder* (Springer-Verlag, Berlin/Gottingen/Heidelberg, 1957).

[24] C. Flammer, The vector wave function solution of the diffraction of electromagnetic waves by circular disks and apertures. II. The diffraction problems, J. Appl. Phys. **24**, 1224 (1953).

[25] C. Flammer, *Spheroidal Wave Functions* (Stanford University Press, Stanford, CA, 1957).

[26] J. D. Jackson, *Classical Electrodynamics*, 3rd ed. (Wiley, New York, 1999).

[27] L. A. Vainstein, *Electromagnetic Waves* (Radio i Svyaz, Moscow, 1988) (In Russian).

[28] M. G. Belkina and L. A. Vainstein, *Diffraction of Electromagnetic Waves on Certain Bodies of Revolution* (Soviet Radio, Moscow, 1957) (In Russian).

[29] Y. A. Ivanov, *Diffraction of Electromagnetic Waves on Two Bodies* (Nauka i Tekhika, Minsk, 1968) (In Russian). Translated by National Aeronautics and Space Administration Washington, D.C., April 1970, https://archive.org/details/nasa_techdoc_19700016001.

[30] *Handbook of Mathematical Functions With Formulas, Graphs, and Mathematical Tables*, edited by M. Abramowitz and I. A. Stegun (National Bureau of Standards, Washington, D.C., 1972).

[31] I. V. Komarov, L. I. Ponomarev, and S. Y. Slavyanov, *Spheroidal and Coulomb Spheroidal Functions* (Nauka, Moscow, 1976) (In Russian).